INSTITUTE OF PHYSICS PUBLISHING JOURNAL OF PHYSICS: CONDENSED MATTER

J. Phys.: Condens. Matter **18** (2006) S963–S968 doi:10.1088/0953-8984/18/25/S04

Strength, anisotropy, and preferred orientation of solid argon at high pressures

Ho-kwang Mao[1], James Badro[2], Jinfu Shu[1], Russell J Hemley[1] and Anil K Singh[3]

[1] Geophysical Laboratory, Carnegie Institution of Washington, 5251 Broad Branch Road, NW, Washington, DC 20015, USA
[2] Laboratoire de Minéralogie-Cristallographie, Institut de Physique du Globe de Paris, Université Pierre et Marie Curie, 140 rue de Lourmel, 75015 Paris, France
[3] Materials Science Division, National Aerospace Laboratories, Bangalore 560017, India

E-mail: mao@gl.ciw.edu

Received 7 May 2006
Published 8 June 2006
Online at stacks.iop.org/JPhysCM/18/S963

Abstract

The elasticity and plasticity of materials at high pressure are of great importance for the fundamental insight they provide on bonding properties in dense matter and for applications ranging from geophysics to materials technology. We studied pressure-solidified argon with a boron–epoxy–beryllium composite gasket in a diamond anvil cell (DAC). Employing monochromatic synchrotron x-radiation and imaging plates in a radial diffraction geometry (Singh *et al* 1998 *Phys. Rev. Lett.* **80** 2157; Mao *et al* 1998 *Nature* **396** 741), we observed low strength in solid argon below 20 GPa, but the strength increases drastically with applied pressure, such that at 55 GPa, the shear strength exceeded 2.7 GPa. The elastic anisotropy at 55 GPa was four times higher than the extrapolated value from 30 GPa. Extensive (111) slip develops under uniaxial compression, as manifested by the preferred crystallographic orientation of (220) in the compression direction. These macroscopic properties reflect basic changes in van der Waals bondings under ultrahigh pressures.

1. Introduction

The application of very high pressures can impart fundamental changes in the bonding characteristics of materials, thus altering their mechanical properties. The pressure effect on mechanical strength is still a poorly understood property which is difficult to predict theoretically [3] at high pressures. With the pressure gradient method [4] and the radial x-ray diffraction method [2, 5], the shear strength of solids can be measured in a DAC to hundreds of GPa. The shear strengths of most materials with metallic, ionic, and covalent bonding, such as Fe [6, 7] Re [8], NaCl [9, 10], MgO [10–13], Al_2O_3 [14], B_6O [15], pyrite [16], ringwoodite [17, 18], and perovskites [19, 20], increase linearly or sub-linearly

with increasing pressures. Materials often soften at pressure-induced phase transformations, such as in the examples of coordination changes in amorphous SiO_2 [21], stishovite-$CaCl_2$ structural transition in SiO_2 [22], and B1–B2 transition in NaCl [9], but can also harden drastically at a major bonding change, such as in the example of cold compressed graphite [23] and BN [24]. Noble gas solids with van der Waals-type bonding are often regarded as very weak, and therefore are used as quasi-hydrostatic pressure transmitting media in high-pressure experiments (for example, [25, 26]). Pressure-induced hardening of noble gas solids has been reported at high pressures [27, 28], but these studies have been limited to indirect observations of pressure gradient or the broadening of x-ray diffraction peaks of samples imbedded in the media. Here we report the quantitative determination of the strength of solid argon as a function of pressure up to 55 GPa using radial x-ray diffraction in a DAC.

2. Experiments

To acquire the high resolution necessary for differentiating the small strain in argon, we employed the angular dispersive x-ray diffraction (ADXD) technique with 33.169 keV monochromatic x-radiation (calibrated with the iodine K edge) with the Fastscan imaging plate system at the ID30 undulator beamline of the European Synchrotron Radiation Facility (ESRF). Complete diffraction rings were obtained from the same sample volume simultaneously, thus eliminating the uncertainties associated with pressure gradients and drift in energy-dispersive x-ray diffraction studies [2]. The incident x-ray is normal to the compression axis and passes through the 5 mm diameter of the 1 mm thick disc-shaped beryllium gasket. To avoid the background diffraction from the 5 mm-thick Be gasket overwhelming the diffraction of the tiny (60 μm) Ar sample, we drilled 200 μm-diameter holes from both sides of the Be gasket to remove 4.5 mm of the 5 mm Be along the x-ray beam path and refilled the holes with amorphous boron epoxy to maintain the support [19]. Diffraction rings from the remaining 500 μm Be in the x-ray path have comparable intensities to those of the 60 μm-deep Ar but do not overlap with the Ar rings (figure 1), thus serving as a useful reference. Diffraction patterns at 13, 28, 40, and 55 GPa were collected and processed with the Fit2d code [29].

3. Results

The sample is subjected to two stress components in the DAC: axial (σ_3) and radial (σ_1) stresses. The average pressure is

$$P = (\sigma_3 + 2\sigma_1)/3 \tag{1}$$

and the deviatoric stress is

$$t = \sigma_3 - \sigma_1 \tag{2}$$

which is also the lower bound of the shear strength. In the ADXD geometry, the azimuth angle (φ) of the DAC, where the DAC compression axis is at $\varphi = 0°$ and 180°, is related to the azimuth angle (α) of an x-ray diffraction ring with a 2θ diffraction angle, where the projection of the DAC compression axis on the imaging plate is at $\alpha = 0°$ and 180°, by

$$\cos\varphi = \cos\theta \cos\alpha. \tag{3}$$

Under the deviatoric stress, Ar shows a strong preferred orientation. Most notably, the (220) diffraction intensity is strongest at $\alpha = 0°$ and 180° (the compression axis), and the (200) diffraction intensity shows maxima at $\alpha = 45°$, 135°, 225° and 315° (figure 1). This indicates that the van der Waals-bonded solid Ar deforms by (111) slip, similarly to metallic-bonded fcc

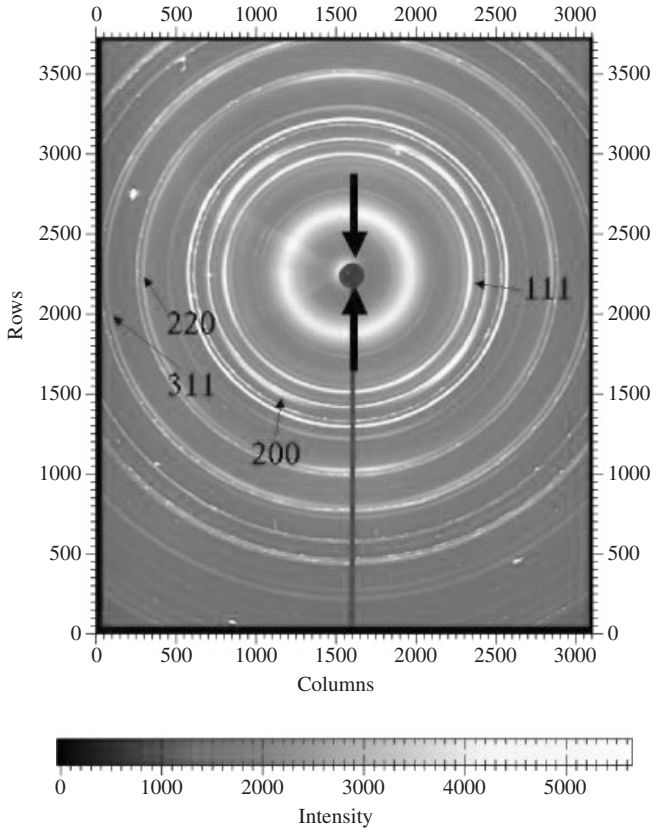

Figure 1. Diffraction pattern recorded by Fastscan imaging plate system at 55 GPa. The compression axis is shown as thick arrows. Four argon rings and their indices (*hkl*) are labelled and indicated by arrows. All other rings are from the Be gasket or boron epoxy filler. The dark circle at the centre and the vertical line below are the shadow of the x-ray beam stop and the supporting wire at $\alpha = 180°$. The argon rings show strong ellipticity and preferred orientation. For instance, the Ar (220) ring is much closer to the circular Be ring immediately outside (the adjacent Ar and Be rings appearing as a doublet) at $\alpha = 0°$ and 180° than at 90° and 270°, indicating the elongation of the Ar ellipse toward 0° and 180° (the compression axis).

metals [30]. This also explains why Ar (200) and (220) reflections are often weak or absent in comparison to the (111) reflection when Ar is used as a pressure medium in routine axial x-ray diffraction experiments ($\alpha = 90° \pm 10°$) at the HPCAT, Sector 16 beamline of the Advanced Photon Sources, Argonne National Laboratory.

Below 20 GPa, Ar diffraction rings are nearly circular; at higher pressures, they become increasingly elliptical. At 55 GPa, the Ar rings are visibly elliptical in comparison to the neighbouring circular Be ring (figure 1). The observed ellipticity indicates a dramatic increase in the Ar strength. As shown in figure 2, the ellipse can be expressed as a trigonometric function of d-spacing and φ

$$d = d_{\mathrm{P}}[1 + (1 - 3\cos^2\varphi)\,Q] \tag{4}$$

where the slope Q indicates the magnitude of the differential strain [1]. The bulk shear strength of Ar can be obtained from

$$t = 6G\langle Q\rangle \tag{5}$$

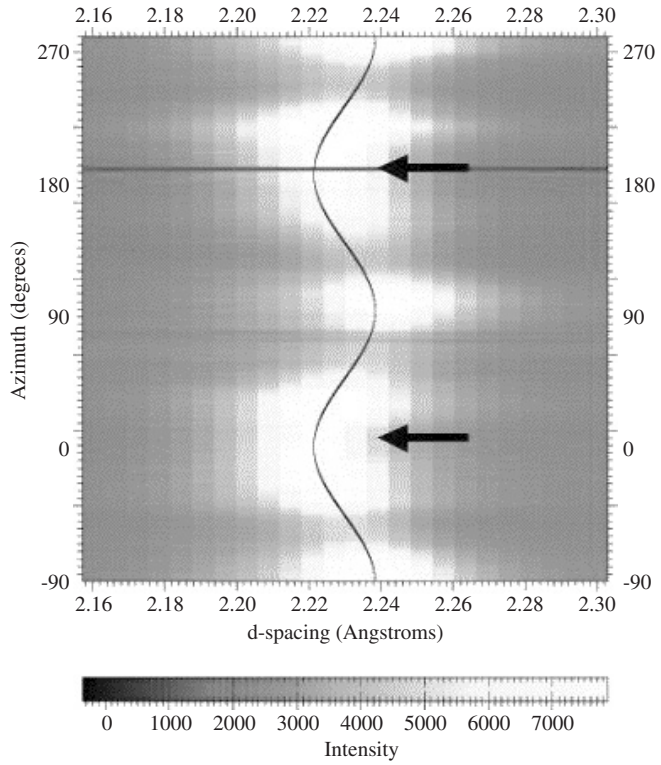

Figure 2. Diffraction ring of Ar (111) converted to Cartesian coordination of d-spacings versus azimuth angle α. The compression directions at 0° and 180° are shown as thick arrows.

where $\langle Q \rangle$ denotes the average $Q(hkl)$, and G is the shear modulus from the Brillouin data [31]. The values of t are initially very low, but increase superlinearly with pressure (figure 3); the $\Delta t/\Delta P$ is 0.02 between 13 and 28 GPa, but increases to 0.08 between 40 and 55 GPa. The relation fits a parabolic function:

$$t\,(\text{GPa}) = 0.001\,P^2 - 0.01\,P. \tag{6}$$

At 55 GPa, t for Ar reaches 2.7 GPa, which exceeds the strength of hardened steel at ambient conditions. The astonishing superstrength of Ar above 30 GPa reflects major changes in the van der Waals bonding.

The degree of ellipticity of the diffraction rings is also a function of the crystallographic orientation. As shown in figure 2, the d-spacing varies by as much as 0.7% between axial ($\alpha = 0°$) and radial ($\alpha = 90°$) directions for the Ar(111) plane, and 1.3% for Ar (200). For cubic crystals [1], the hkl dependence of Q can be expressed as a linear function of B (figure 4), where $B = 3(h^2k^2 + k^2l^2 + l^2h^2)/(h^2 + k^2 + l^2)^2$ denotes the orientation, and $A = (2c_{44})^{-1} - (c_{11} - c_{12})^{-1}$ denotes the elastic anisotropy.

$$Q = m_0 + m_1 B \tag{7}$$

$$3m_1 = t[(2c_{44})^{-1} - (c_{11} - c_{12})^{-1}]. \tag{8}$$

The observed $m_1 = -2\times10^{-3}$ at 55 GPa is considerably larger than $m_1 = -5\times10^{-4}$ calculated using extrapolated c_{ij} values from Brillouin spectroscopy measurements up to 30 GPa [31], indicating significant changes of bonding at high pressures.

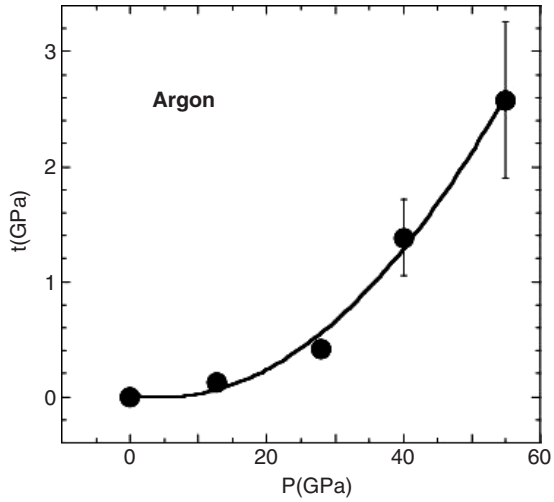

Figure 3. Deviatoric stress, which is the lower bound of the strength, of Ar as a function of pressure. The vertical bars indicate the range at different crystallographic orientation (*hkl*). The true error bars are significantly smaller.

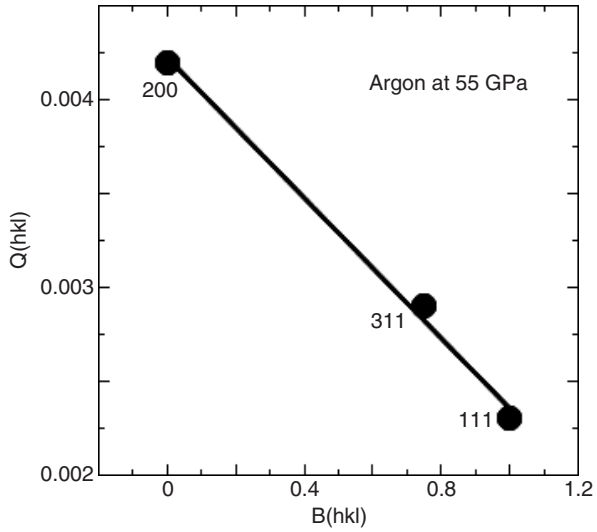

Figure 4. Differential strain of Ar at 55 GPa as a function of $B(hkl)$.

4. Conclusion

In conclusion, the present observations of pressure-induced strength and elastic anisotropy in solid argon reveal drastic changes of van der Waals bondings that dictate the structure and chemistry of noble gas elements at high pressures. For instance, the melting temperatures of argon and xenon increase steeply with pressure and exceed that of iron at 30 GPa [32]. The present observations provide valuable constraints on the theoretical understanding of the behaviour of simple solids at high densities, including the evolution of many-body effects with compression [33, 34].

Acknowledgments

We thank Haozhe Liu and Hans-Rudolf Wenk for valuable comments and Tristan LeBihan for help at the synchrotron beamline. The synchrotron facilities are supported by the ESRF. Support was provided by National Science Foundation-Earth Sciences (NSF-EAR), Department of Energy-Basic Energy Sciences (DOE-BES) (HPCAT), DOE-National Nuclear Security Administration (NNSA) (Carnegie/DOE Alliance Center), and the W M Keck Foundation of the United States and CNRS of France. Laboratoire de Minéralogie-Cristallographie is CNRS UMR 7590.

References

[1] Singh A K, Mao H K, Shu J and Hemley R J 1998 *Phys. Rev. Lett.* **80** 2157
[2] Mao H K, Shu J, Shen G, Hemley R J, Li B and Singh A K 1998 *Nature* **396** 741
[3] Söderlind P, Yang L H, Moriarty J A and Wills J M 2000 *Phys. Rev.* B **61** 2579
[4] Sung C-M, Goetze C and Mao H K 1977 *Rev. Sci. Instrum.* **48** 1386
[5] Kinsland G L and Bassett W A 1976 *Rev. Sci. Instrum.* **47** 130
[6] Hemley R J, Mao H K, Shen G, Badro J, Gillet P, Hanfland M and Häusermann D 1997 *Science* **276** 1242
[7] Merkel S, Shu J, Gillet P, Mao H K and Hemley R J 2005 *J. Geophys. Res.* **110** B025201
[8] Jeanloz R, Godwal B K and Meade C 1991 *Nature* **349** 687
[9] Meade C and Jeanloz R 1988 *J. Geophys. Res.* **93** 3270
[10] Kinsland G L and Bassett W A 1977 *J. Appl. Phys.* **48** 978
[11] Meade C and Jeanloz R 1988 *J. Geophys. Res.* **93** 3261
[12] Duffy T S, Hemley R J and Mao H K 1995 *Phys. Rev. Lett.* **74** 1371
[13] Merkel S, Wenk H R, Shu J, Shen G, Gillet P, Mao H K and Hemley R J 2002 *J. Geophys. Res.* **107** doi:10.1029/2001JB000920
[14] Meade C and Jeanloz R 1990 *Phys. Rev.* B **42** 2532
[15] He D, Shieh S R and Duffy T S 2004 *Phys. Rev.* B **70** 184121
[16] Merkel S, Jephcoat A P, Shu J, Mao H K, Gillet P and Hemley R J 2002 *Phys. Chem. Miner.* **29** 1
[17] Kavner A and Duffy T S 2001 *Geophys. Res. Lett.* **28** 2691
[18] Kavner A 2003 *Earth Planet. Sci. Lett.* **214** 645
[19] Merkel S, Wenk H R, Badro J, Montagnac G, Gillet P, Mao H K and Hemley R J 2003 *Earth Planet. Sci. Lett.* **209** 351
[20] Shieh S R, Duffy T and Shen G 2004 *Phys. Earth Planet. Inter.* **143** 93
[21] Meade C and Jeanloz R 1988 *Science* **241** 1072
[22] Shieh S R, Duffy T S and Li B 2002 *Phys. Rev. Lett.* **89** 255507
[23] Mao W L, Mao H K, Eng P, Trainor T, Newville M, Kao C C, Heinz D L, Shu J, Meng Y and Hemley R J 2003 *Science* **302** 425
[24] Meng Y, Mao H K, Eng P, Trainor T, Newville M, Hu M Y, Kao C C, Häusermann D and Hemley R J 2004 *Nat. Mater.* **3** 111
[25] Errandonea D, Boehler R and Ross M 2002 *Phys. Rev.* B **65** 012108
[26] Chudinovskikh L and Boehler R 2001 *Nature* **411** 574
[27] Bell P M and Mao H K 1981 *Carnegie Inst. Washington Yearb.* **80** 404
[28] Takemura K 2001 *J. Appl. Phys.* **89** 662
[29] Hammersley J 1996 *ESRF Report* No. ESRF98HAO1T
[30] Wenk H-R, Lonardelli I, Pehl J, Devine J, Prakapenka V, Shen G and Mao H K 2004 *Earth Planet. Sci. Lett.* **226** 507
[31] Grimsditch M, Loubeyre P and Polian A 1986 *Phys. Rev.* B **33** 7192
[32] Jephcoat A P 1998 *Nature* **393** 355
[33] Datchi F, Loubeyre P and LeToullec R 2000 *Phys. Rev.* B **61** 6535
[34] Occelli F, Krisch M, Loubeyre P, Sette F, Toullec R L, Masciovecchio C and Rueff J-P 2001 *Phys. Rev.* B **63** 224306